International Copper Association
Copper Alliance

Final Report

PROJECTS TEK-1064-SJTU and MDP-1268-HA

August 2014 – August 2016

Ultra-Conductive Copper Development in China

Consultant & Project Manager:
Dr. Horst Adams, Adamco Inc., 2223 Watts Street, Houston TX, 77030

Executing Lab:
State Key Laboratory of Metal Matrix Composites, Shanghai Jiao Tong University, Shanghai 200240, People's Republic of China

ABSTRACT

This final report summarizes the concluding results obtained in the ICA projects *TEK-1064-SJTU* and *MDP-1268-HA* during the total project duration from August, 2014 to August, 2016. The main goal of the final project phase was to fabricate, investigate, and explain the behavior of copper / graphene nanocomposite material with an electrical conductivity of >= 114% IACS.

Results:

1. Lab samples of graphene/copper composite material with a dimension of 20 × 20 × 1 mm^3 have been fabricated, in which an electrical conductivity of up to ~116% IACS could be reproducibly achieved (verified by Argonne National Lab and General Cable Inc.)
2. Short wires with a length > 30 mm have been made with the same conductivity.
3. The morphology, texture and electrical current distribution across of the Gr/Cu interface have been studied.
4. A theoretical approach to explain the increased conductivity has been developed.

Amendment 1: As a proposal for a follow-up project, a possible way to mass produce graphene loaded copper is proposed.

Introduction

Every year more than ten million tons of copper are used for electrical and electronic purpose in the world, as it is the most cost-effective and reliable electrically conductive material for many applications and second only to silver in its ability to conduct electricity. However, even higher electrical conductivity than that of copper is desired because of increasing demands on more efficient electrical power and signal transmission, less heat generation and faster heat dissipation in devices, which means reductions in energy consumption and benefits for downscaled electronics. Extensive research efforts have been dedicated to improving the electrical conductivity of copper, such as producing copper with a purity as high as 7N or oxygen content as low as 1×10^{-4} %, but an improvement of only ~3% has been achieved in this highly refined copper since the electrical conductivity of copper was first officially recorded about 100 years ago.

Graphene (Gr), a one-atom-thick two dimensional carbon material, is highly promising for electrical,[1-3] thermal[4,5] and mechanical[6] applications. As an ideal reinforcement in composite materials,[7,8] graphene has proven to be very effective in enhancing mechanical properties of metals,[9-11] but its theoretical ability to improve electrical conductivity of bulk metals is yet to be verified experimentally. Graphene is known to have a remarkable electron mobility, reaching a value exceeding 200,000 $cm^2\ V^{-1}\ s^{-1}$ at electron densities of $\sim2\times10^{11}\ cm^{-2}$ in a suspended single layer graphene sheet.[12] And according to some recent reports, the electrical and thermal benefits of graphene capping on both micro- and nanoscale Cu wires,[13,14] are mainly attributed to the significant reduction in surface scattering of electrons. However, these properties cannot be simply extended to bulk graphene-Cu composites due to the markedly different behavior of graphene embedded in a matrix and graphene with a free surface. For example, graphene is known to have a high intrinsic thermal conductivity, which can reach a level of $K \approx 5{,}000\ W\ m^{-1}K^{-1}$ at room temperature in suspended and sufficiently large high-quality samples.[4,5] However, graphene deposition on substrates results in a degradation of thermal conductivity to ~600 $W\ m^{-1}\ K^{-1}$ due to phonon scattering at the substrate defects and at the interface.[15]

Scope of work

In this work we fabricated a Gr/Cu multilayered composite as a model to explore the possible role of graphene on improving the electrical conductivity of copper by chemical vapor deposition (CVD) of graphene on both sides of micrometer-scale Cu foils and then hot-pressing a multitude of the as-obtained Gr-Cu-Gr heterogeneous foils together to form bulk samples of highly conductive composite material. Our electrical measurements demonstrate that introducing graphene into the Cu matrix results in ultrahigh interface- and bulk electrical conductivity in the resulting Gr/Cu multilayered composite, with an interface conductivity of three orders of magnitude higher than the conductivity of the pure Cu matrix, and a bulk electrical conductivity of up to 16% higher than that of Cu. Our experimental results and first-principles calculations suggest that the ultrahigh interfacial and bulk conductivities are primarily due to graphene-promoted changes in the Cu morphology and crystallinity, as well as electron doping effects on graphene caused by the Cu matrix. The ultrahigh electrical conductivity shows the potential to

have a significant impact on a wide range of applications of Cu for electrically and thermally conducting purposes. The relationship between electrical conductivity enhancement and interface properties as well as the matrix microstructure are of significance for designing advanced Cu-based materials with ultrahigh electrical conductivity and strength, which could be achieved in Gr/Cu nanolayered composites because of the markedly increased volume fraction of such ultrahigh conductive interfacial layers, coupled with the as-demonstrated outstanding strengthening effect of graphene in metals [11].

Sample Preparation

Figure 1 shows a schematic of the sample preparation. The Gr/Cu multilayered composites were fabricated by CVD of graphene on both sides of 30-μm thick Cu foils and then hot-pressing five pieces of the resulting Gr-Cu-Gr heterogeneous foil into a 150-μm thick sheet.

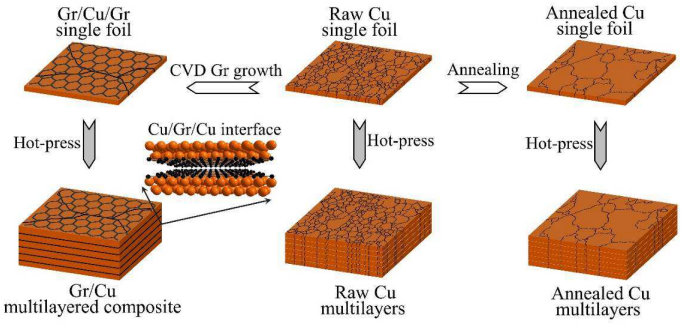

Figure 1. Schematic of sample fabrication.

Graphene was deposited on both sides of a pristine Cu foil by chemical vapor deposition. Pristine Cu, annealed under the same condition without graphene deposition, was also prepared as a reference sample. For each sample, several pieces of single foil were stacked and then transformed into thicker sheet by a hot-pressing process.

The number of atomic planes in the graphene films on the Cu foil was verified with Raman spectroscopy, and the I_{2D}/I_G ratio of about 2.3 indicated that the deposited graphene on the Cu foils was mostly single layered (see Figure S1 in the Supporting Information).[16] Therefore, the interfaces in the Gr/Cu multilayered composites were composed of Cu/Gr bilayer/Cu because of the stacked Gr-Cu-Gr multilayers. For reference we also prepared two other sample types from a) pristine Cu foils ("as rolled") without graphene or any thermal treatment, and b) Cu foils annealed under the same temperature as the one used during CVD of graphene but without graphene deposition (see Figure S2 in the Supporting Information). Thus, for comparison with the ultraconductive samples, we used hot-pressed multilayers of pristine Cu, and annealed Cu, Gr-Cu-Gr foils, respectively (see Figure S3 in the Supporting Information).

Conductivity Measurement

Figure 2 shows the average electrical conductivities of both single foil, and hot-pressed multilayer samples of:

- pristine Cu,
- annealed Cu and
- Gr/Cu.

The electrical conductivities of the International Annealed Copper Standard (IACS, 58.1×10^6 S m^{-1}) and Ag (~108% IACS) are also shown for comparison.

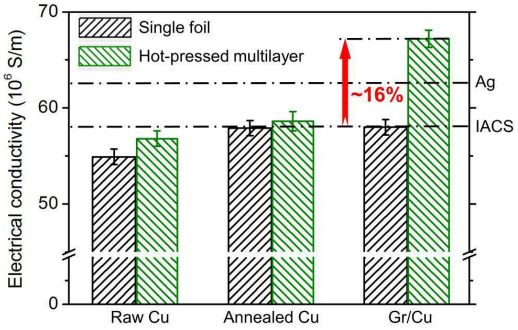

Figure 2. Electrical conductivity characterizations of both single foil and hot-pressed multilayer samples of:

pristine Cu (left columns),
annealed Cu (middle columns) and
Gr/Cu (right columns).

The electrical conductivity of the International Annealed Copper Standard (IACS) and Ag (108% IACS) are shown for comparison.

Using a standard four-probe method (see Figure S4 in the Supporting Information), the electrical conductivity of the pristine Cu single foil was measured to be 54.9×10^6 S m^{-1} (94.7% IACS); the conductivity increased to 57.9×10^6 S m^{-1} by annealing the Cu sample, and reached 58×10^6 S m^{-1} by the deposition of graphene on the Cu surface, approaching but not exceeding the 100% IACS level. While the hot-pressing process could further slightly raise the electrical conductivity by 2.8% IACS in the pristine Cu multilayer and by 1% IACS in the annealed Cu multilayer, a significant enhancement of up to 16% IACS and an ultrahigh bulk electrical conductivity of 67.2×10^6 S m^{-1} was obtained in the Cu/Gr-Gr/Cu multilayered composites, which is even higher than that of the best conductive metal Ag.

Conductivity Determining Factors

Electron scattering on grain boundaries is a main factor of electrical resistivity. To investigate the Cu morphology evolution after the different processing procedures, analyses of the grain size distribution and surface texture were carried out by electron backscattered diffraction (EBSD) on the single foils of pristine Cu, annealed Cu, and Gr-Cu-Gr respectively. **Figure 3** shows that the annealing treatment resulted in remarkable grain growth in the single foils because the processing temperature of 1,000ºC is sufficiently higher than the Cu recrystallization temperature of ~227ºC.[17]

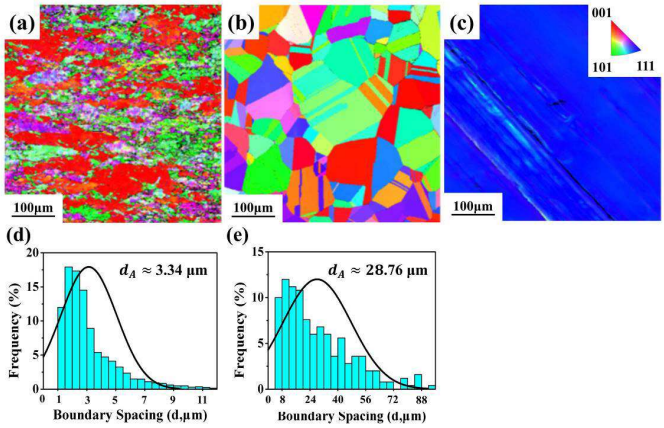

Figure 3. Texture analysis by inverse pole figure (IPF) map and grain size statistics based on EBSD for the single foils of (a,d) pristine Cu, (b,e) annealed Cu, and (c) Gr/Cu/Gr.

As a consequence, the low electrical conductivity of pristine Cu single foils can be explained by grain refinement during its rolling fabrication process, while the conductivity recovered up to the level of 100% IACS after annealing due to grain coarsening. Moreover, chemical vapor deposition of graphene on the Cu surface results in an even substantially stronger enlargement of the Cu grains than that caused by the annealing treatment under the same temperature conditions. We also observed that a grain reorientation took place during CVD of graphene. However, compared to the annealing treatment these stronger changes in grain size and orientation during CVD of graphene did not lead to any additional enhancement of the electrical conductivity of the individual foils.

Goli *et al* demonstrated an increase of thermal conductivity by 16~24% in CVD-Gr/Cu/CVD-Gr heterogeneous foils as compared to the reference pristine Cu and annealed Cu, which was primarily arising from the changes of Cu morphology and the strong enlargement of Cu grains during CVD of graphene.[18] However, the electrical conductivities of their samples were in line with the standard values for Cu foils, and did not scale up linearly with the increased thermal conductivity as predicted by the Wiedemann-Franz law[19] $K/\sigma = LT$, where K is the thermal conductivity, σ is the electrical conductivity and $L = (\pi^2/3)(\kappa_B/q)^2 \approx 2.44 \times 10^{-8}$ $W\Omega K^{-2}$ is the Lorenz number. These results are consistent with our findings that CVD of graphene on both sides of a several tens of micrometers thick Cu foil did not lead to any additional electrical conductivity compared to a Cu foil annealed under the same conditions but without graphene deposition.

Additionally, the thickness of the graphene layer $h = 0.34$ nm is negligibly small compared to that of the Cu foil $H = 30$ μm, and also H is much larger than the electron mean free path in Cu (40 nm at 298 K).[20] Therefore the reduction in surface scattering of electrons by surface graphene layers demonstrated in nanomaterials is negligible here.

In order to exclude any possible influence of impurities on the electrical conductivity, we also performed X-ray photoelectron spectroscopy (XPS) and energy-dispersive X-ray (EDX) spectroscopy analyses on Gr-Cu-Gr single foils and reference annealed Cu single foils, revealing that there is no perceivable difference in the impurity contents, including O and N, between the two single foil types (see Figure S5 in the Supporting Information).

Conductivity of Stacked and Hot-Pressed Samples

Although the strong enlargement and reorientation of Cu grains after CVD of graphene did not lead to any direct advantages over the annealing treatment on improving the electrical conductivity of single Cu foils, both effects proved to be beneficial for enhancing crystallinity and thus electrical conductivity in Gr-Cu multilayered composites produced by hot-pressing several single layer samples together. High-resolution X-ray diffraction pole figures showed that, with the hot-pressing treatment, the intensity of the main peak Cu(111) was enhanced in the hot-pressed Gr-Cu multilayered composite, while the additional small Cu(200) and other peaks caused by weakly tilted orientation states in the single Gr-Cu-Gr foil were attenuated, suggesting that an enhancement of the preferred texture and crystallinity might be responsible for enhancing the electrical conductivity in Gr-Cu multilayered composites (see Figure S6 in the Supporting Information).

Ajmal *et al* reported that hot isostatic pressing of a single-crystal Cu sample could increase the electrical conductivity by 5.5% because of the increased crystallinity.[21]

In our work, an enhancement of up to 16% was obtained, and we think, that graphene CVD might have contributed in promoting grain reorientation and curing grain boundaries during the hot-pressing process because of the matching lattice constants of graphene (2.46 Å) and Cu(111) (2.56 Å).[22,23] The atomic spacing in the Cu(111) direction is within 4% of the graphene lattice constant, which is why the connection between graphene and copper works so well. We think, the C-atom lattice of the graphene film attached to the thin Cu-foil acts as a seed-structure or template for the preferred re-orientation of the Cu(111) grain plane toward the graphene layer during the hot pressing process. This in turn causes the formation of an abundance of electron transfer tunnels between the electron sea with high mean free path of the closely matching Cu(111) plane and the Pi-orbitals of the C-atoms in the graphene lattice.

Table 1 shows the room temperature crystal structures for several metals commonly used in industrial applications. The listed metals have respective unit cell structures described as body center cubic (bcc), face centered cubic (fcc), or hexagonal close packed (hcp). The table is sorted by the mismatch percentage between the graphene lattice constant and the atomic spacing of the preferred plane in the respective metal. Only four different metals (Fe, Ni, Cr, Co) show better lattice matches than Cu, none of which has any potential to be used as electrical conductor in industrial applications. However, the metals with a mismatch <4% (in particular Fe, Co, Cu) are the of course the preferred catalysts used for the formation of nanocarbons including carbon nanotubes.

metal	crystal structure	atomic spacing (nm)	mismatch (+/- %)
Iron (Alpha)	BCC	0.2482	0.9
Nickel	FCC	0.2492	1.3
Chromium	BCC	0.2498	1.5
Cobalt(Alpha)	HCP	0.2506	1.9
Cobalt(Beta)	FCC	0.2506	1.9
Copper	FCC	0.2556	3.9
Iron (Gamma)	FCC	0.2576	4.7
Vanadium	BCC	0.2622	6.6
Ruthenium	HCP	0.2650	7.7
Zinc	HCP	0.2664	8.3
Osmium	HCP	0.2676	8.8
Rhodium	FCC	0.2690	9.3
Iridium	FCC	0.2700	9.8
Beryllium	HCP	0.2226	-10.5
Molybdenum	BCC	0.2726	10.8
Rhenium	HCP	0.2740	11.4
Palladium	FCC	0.2740	11.4
Tungsten	BCC	0.2742	11.5
Platinum	FCC	0.2776	12.8
Titanium (Beta)	BCC	0.2858	16.2
Niobium	BCC	0.2858	16.2
Tantalum	BCC	0.2860	16.3
Aluminum	FCC	0.2868	16.6
Gold	FCC	0.2884	17.2
Silver	FCC	0.2888	17.4
Titanium (Alpha)	HCP	0.2890	17.5
Cadmium	HCP	0.2978	21.5
Zirconium(Beta)	BCC	0.3124	27.0
Zirconium(Alpha)	HCP	0.3170	28.9
Magnesium	HCP	0.3198	30.0
Lead	FCC	0.3500	42.3

We think that these relations make copper, in particular in the special setup Cu-Gr-Gr-Cu we found to provide the highest conductivity, the ideal candidate to form the above mentioned easy-electron-path tunnels between the graphene layer and the copper matrix and thus can act as an ultraconductive composite material in combination with graphene. Other metals frequently used in conventional cable applications, like aluminum and magnesium, have a mismatch which is too big to allow for a comparably easy electron transfer between the metal and the carbon lattice. We think that this is not only true for the combination of the respective metal with graphene but equally valid for the combination with other C-structures like carbon nanotubes.

Contribution of the Individual Layers to Conductivity

The interface between the additive (in this case graphene) and the matrix material (Cu) has a major effect on the electrical and thermal conductivity of the composite material. To evaluate the electrical properties of the interfaces between the different layers, the electrical conductivity of a selected area across the Cu/Gr-Gr/Cu interface area was investigated by using the contact-current mode of a scanning probe microscope under an applied voltage of 100 mV at room temperature (see Figure S8 in the Supporting Information).

One surface of a Gr/Cu multilayered composite sample was attached (and electrically connected) to the sample stage, while a Pt-coated Si-cantilever with the applied voltage was positioned on the opposite surface. A typical current-mapping image produced by scanning the cantilever probe inside the electron-microscope across the different layers is shown in **Figure 4.**

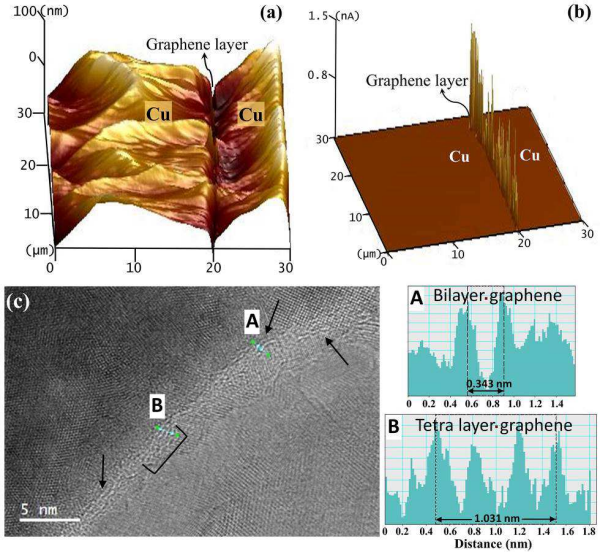

Figure 4: Characterization of Cu/graphene layer/Cu interface by atomic force microscopy.
(a) interface morphology and
(b) typical current-mapping image generated by using the contact-current mode of an atomic force microscopy. The graph plots the current flow across a 30um x 30um mapping area containing a single graphene edge. The current flow in the region of the sandwiched graphene is up to 3 orders of magnitude higher than in the pure Cu area.
(c) TEM image of a graphene-Cu interface that shows mostly bilayer graphene with some tri- and tetralayer graphene. Two high-intensity peaks separated by the expected interplanar spacing of 0.343 nm were observed in region (A) (marked with arrows), whereas four high-intensity peaks were observed in region (B) (marked with line segment).

The measuring area covered 30µm×30µm on the cross section. The electrical current drastically increases at each graphene (double) layer to values about three orders of magnitude higher than at the surrounding Cu matrix. The fluctuations observed in the electrical current might be caused by the polycrystalline and discontinuous nature of the deposited graphene (see Figures S1 in the Supporting Information).

Detailed cross-sectional transmission electron microscopy (TEM) images and histograms of line scans across the interface are shown in Figure 4c; the images indicate the presence of interfaces with both bilayer (region (A)) and tetralayer graphene (region (B)).

Although the volume fraction of the highly conductive graphene interface in the here fabricated Cu/Gr-Gr/Cu multilayered composites is very small (less than 1/30,000 as estimated from the thickness of the graphene layer and Cu foil) and thus their contribution to the enhanced electrical conductivity is still limited (currently 16%), the Cu/Gr-Gr/Cu interface provides a model for preparing ultra-conductive Gr/Cu composites. We think that, by increasing the volume fraction of Cu/Gr-Gr/Cu layers in the bulk composite, the conductivity could be increased much further, with the above measured conductivity across the Gr-Gr layer (orders of magnitude higher than pristine Cu) being the theoretical limit. Also, a nanolayered structure with a

multitude of Gr-Cu interfaces, which could be obtained using the bioinspired route established by us for metal matrix composites (see Figure S9 in the Supporting Information)[24-26] could be used to fabricate bulk ultraconductive Cu / Gr composites.

The Role of Graphene in the Multilayer Composite

In order to better understand the origin of the large enhancement of the interface conductivity, a study of the role of graphene in the composite on an atomic level was performed using first-principles calculations based on a practical model of a Cu/Gr bilayer/Cu interface (see Figure S10 in the Supporting Information). We found that, on average, a primitive cell of the bilayer graphene (containing four carbon atoms) obtains about 0.24 electrons (Table S1) from the neighboring Cu atoms in the matrix, indicating a doping effect in the graphene with an estimated electron density of $\sim 1\times10^{12}$ cm^{-2}. Moreover, as can be seen from the band structure and density of the states for the doped bilayer graphene (**Figure 5**), the Fermi energy is shifted upwards by about 0.54 eV from the Dirac point due to the electron doping, as compared to the pristine bilayer graphene.

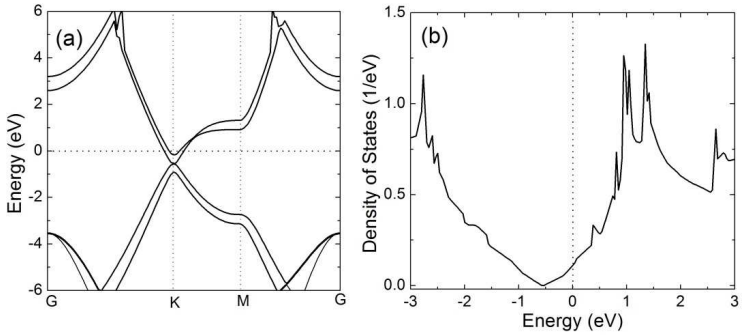

Figure 5.
(a) Band structure and (b) density of states for the doped AB-bilayer graphene. The zero point denotes the Fermi energy.

Effective doping has been previously reported in graphene on metal substrates,[27-29] which could result in a comparable but lower energy shift of the Fermi energy (0.3 eV above the Dirac point) of graphene on a Cu substrate.[28] The doping electrons in a doped Gr bilayer have large Fermi velocities because of the linear energy dispersion relation near the Dirac points, which leads to a very high carrier mobility of three orders of magnitude higher than in copper. Therefore we think that the significant enhancement of interface conductivity can be explained by the electron doping effect in graphene that results in a largely increased carrier density as well as very high carrier mobility in the graphene, leading to an extreme in-plane electrical transport capability. We also think that the graphene double layer might provide for an advantageous defect compensation effect between the individual graphene lattice structures in case one of the layers is for instance mechanically locally disturbed, polycrystalline, or of otherwise discontinuous nature. Electrons could still flow easily through the second undisturbed layer which is as well connected to the Cu electron sea, however on the opposite side.

Summary

We have demonstrated experimentally that hot pressed Cu/Gr-Gr/Cu multilayered composites possess a strongly enhanced bulk electrical conductivity as compared to the reference

pristine Cu or annealed Cu. An electrical conductivity as high as 116% IACS was achieved in the as-obtained composite at room temperature, which is even higher than that of Ag. The observed improvement of the electrical properties of Gr/Cu composites is primarily caused by:

a) the changes in Cu grain size and orientation caused by CVD of graphene, promoting the curing of grain boundaries and increasing of crystallinity combined with preferred atomic lattice matching between graphene and copper during hot-pressing, and

b) the ultrahigh conductivity of the double layered graphene interface of three orders of magnitude higher than that of the copper matrix.

The effect of graphene is projected to be comparably strong in substantially larger sized bulk Gr/Cu nanolayered composites. A principal way to make these large bulk Gr/Cu nanolayered composites is presented in the Supporting Information section to this paper. Enhancement of the electrical properties of Cu is important for reducing energy consumption and offering benefits for downscaled electronics. Our results indicate that incorporating graphene into a Cu matrix can substantially improve its electrical conductivity up to a level higher than that of the most conductive metal Ag, which may lead to a transformational change in the use of carbon in metallurgy.

Acknowledgements

This work was supported by the International Copper Association, the Natural Science Foundation of China (Nos.51371115, 51131004), the Ministry of Science & Technology of China (973 program, No.2012CB619600), and the Shanghai Science & Technology Committee (Nos.14JC1403300, 14DZ2261204, 15JC1402100, 14520710100).

References

[1]. K.S. Novoselov, A.K. Geim, S.V. Morozov, D. Jiang, Y. Zhang, S.V. Dubonos, I.V. Grigorieva, A.A. Firsov, *Science* **2004**, *306*, 666.

[2]. K.S. Novoselov, A.K. Geim, S.V. Morozov, D. Jiang, M.I. Katsnelson, I.V. Grigorieva, S.V. Dubonos, A.A. Firsov, *Nature* **2005**, *438*, 197.

[3]. Y.B. Zhang, Y.-W. Tan, H.L. Stormer, P. Kim, *Nature* **2005**, *438*, 201.

[4]. S. Ghosh, *Nat. Mater.* **2010**, *9*, 555.

[5]. A.A. Balandin, *Nat. Mater*. **2011**, *10*, 569.

[6]. C. Lee, X. Wei, J.W. Kysar, J. Hone, *Science* **2008**, *321*, 385.

[7]. K.S. Novoselov, V.I. Fal'ko, L. Colombo, P.R. Gellert, M.G. Schwab, K. Kim, *Nature* **2012**, *490*, 192.

[8]. X. Huang, X.Y. Qin, F. Boey, H. Zhang, *Chem. Soc. Rev*. **2012**, *41*, 666.

[9]. D.-B. Xiong, M. Cao, Q. Guo, Z.Q. Tan, G.L. Fan, Z.Q. Li, D. Zhang, *ACS Nano* **2015**, *9*, 6934.

[10]. J. Hwang, T. Yoon, S.H. Jin, J. Lee, T. Kim, S.H. Hong, S. Jeon, *Adv. Mater*. **2013**, *25*, 6724.

[11]. Y. Kim, J. Lee, M.S. Yeom, J.W. Shin, H. Kim, Y. Cui, J.W. Kysar, J. Hone, Y. Jung, S. Jeon, S.M. Han, *Nature Comm*. **2013**, *4*, 2114.

[12]. K.I. Bolotin, K.J. Sikes, Z. Jiang, M. Klima, G. Fudenberg, J. Hone, P. Kim, H.L. Stormer, *Solid State Comm*. **2008**, *146*, 351.

[13]. C.G. Kang, S.K. Lim, S. Lee, S.K. Lee, C. Cho, Y.G. Lee, H.J. Hwang, Y. Kim, H.J. Choi, S.H. Choe, M.-H. Ham, B.H. Lee, *Nanotechnology* **2013**, *24*, 115707.

[14]. R. Mehta, S. Chugh, Z.H. Chen, *Nano Lett*. **2015**, *15*, 2024.

[15]. J.H. Seol, I. Jo, A.L. Moore, L. Lindsay, Z.H. Aitken, M.T. Pettes, X.S. Li, Z. Yao, R. Huang, D. Broido, N. Mingo, R.S. Ruoff, L. Shi, *Science* **2010**, *328*, 213.

[16]. Z.H. Ni, Y.Y. Wang, T. Yu, Z.X. Shen, *Nano Res*. **2008**, *1*, 273.

[17]. R.A. Flinn, P.K. Trojan, *Engineering Materials and Their Application: Effect of Stress and Temperature*; Houghton Mifflin Company: Boston, MA, 1981; Figure 3-26.

[18]. P. Goli, H. Ning, X.S. Li, C.Y. Lu, K.S. Novoselov, A.A. Balandin, *Nano Lett*. **2014**, *14*, 1497.

[19]. R. Franz, G. Wiedemann, *Ann. Phys*. 1853, *165*, 497.

[20]. R.L. Graham, G.B. Alers, T. Mountsier, N. Shamma, S. Dhuey, S. Cabrini, R.H. Geiss, D.T. Read, S. Peddeti, *Appl. Phys. Lett*. **2010**, *96*, 042116.

[21]. M. Ajmal, S. Lee, Y.C. Cho, S.J. Kim, S.E. Park, C.R. Cho, S.-Y. Jeong, *CrystEngComm* **2012**, *14*, 1463.

[22]. L. Gao, J.R. Guest, N.P. Guisinger, *Nano Lett*. **2010**, *10*, 3512.

[23]. L. Zhao, K.T. Rim, H. Zhou, R. He, T.F. Heinz, A. Pinczuk, G.W. Flynn, A.N. Pasupathy, *Solid State Comm*. **2011**, *151*, 509.

[24]. Z. Li, Q. Guo, Z.Q. Li, G.L. Fan, D.-B. Xiong, Y.S. Su, J. Zhang, D. Zhang, *Nano Lett*. **2015**, *15*, 8077.

[25]. Z. Li, G.L. Fan, Z.Q. Tan, Z.Q. Li, Q. Guo, D.-B. Xiong, D. Zhang, *Nano-Micro Lett*. **2016**, *8*, 54.

[26]. J.Y. Wang, Z.Q. Li, G.L. Fan, H.H. Pan, Z.X. Chen, D. Zhang, *Scrip. Mater*. **2012**, *66*, 594.

[27]. A. Dahal, M. Batzill, *Nanoscale*, **2014,** *6*, 2548.

[28]. A. L. Walters, S. Shu, A. Bostwick, K.S. Kim, L. Moreschini, Y.J. Chang, D. Innocenti, K. Horn, K.F. McCarty, E. Rotenberg, *Phys. Rev. B*, **2011**, *84*, 195443.

[29]. P. Sutter, J. T. Sadowski and E. Sutter, *Phys. Rev. B*, **2009**, *80*, 245411.

[30]. G. Kresse, J. Furthmüller, *Phys. Rev. B*, **1996,** *54*, 11169.

[31]. P.E. Blöchl, *Phys. Rev. B*, **1994,** *50*, 17953.

[32]. H.J. Monkhorst, J. D. Pack, *Phys. Rev. B*, **1976**, *13*, 5188.

Supporting Information

Sample Preparation and Characterization

Graphene was deposited on both sides of Cu foils via chemical vapor deposition. In a typical process Cu foils with a thickness of $H \approx 30$ μm were heated up to 1,000ºC in a hydrogen/argon atmosphere and then methane was introduced for graphene growth. The Cu foils were cooled down to room temperature within 30 minutes to grow single layer graphene on both sides of the Cu foil, thus Gr-Cu-Gr foils were obtained (**Figure S1**). The annealing of the pristine ("as rolled") copper reference samples was performed with the same heating and cooling process but without methane addition.

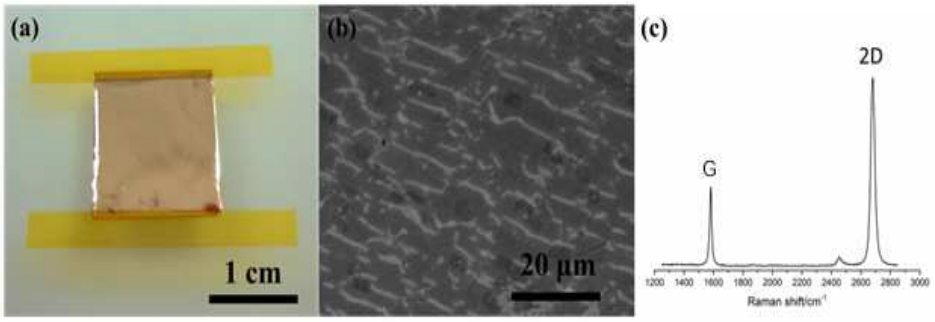

Figure S1 (a) Photograph of a CVD graphene/copper single foil; (b) SEM image of graphene crystals on Cu foil prepared by CVD; the graphene surface coverage is almost 95%; (c) Raman spectroscopy of the deposited graphene which shows that the graphene deposited on the copper surface is a single layer with $I_{2D}/I_G \approx 2.3$.

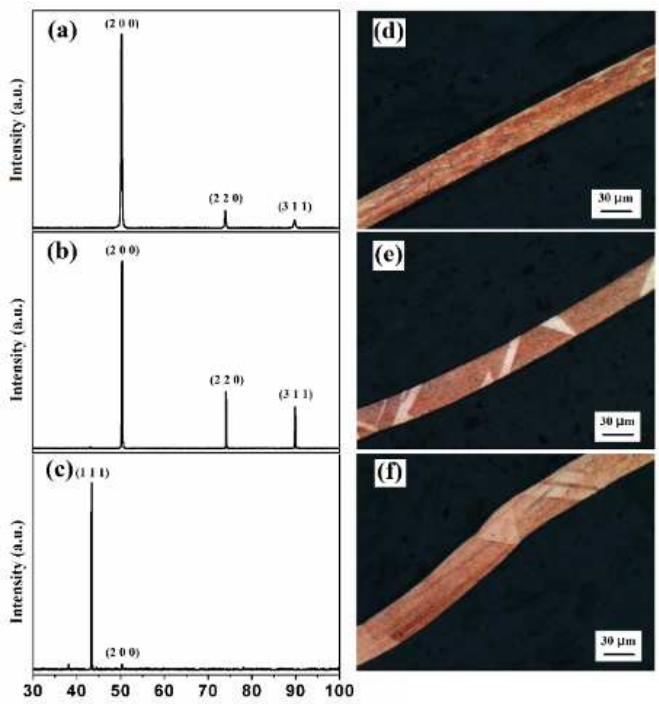

In order to prepare thicker sheet samples, several pieces of Gr-Cu-Gr foil were stacked on top of each other in a graphite mold and then hot-pressed at 900ºC for 20 minutes in an 50 MPa Ar atmosphere. Thick sheet reference samples of pristine Cu and annealed Cu were also prepared under the same hot pressing conditions. The typical thickness of a stacked and sintered sheet sample was about 150 μm.

Figure S2.
In-plane XRD patterns (left) and cross-section optical images (right) of single foils of:
(a,d) pristine Cu,
(b,e) annealed Cu, and
(c,f) Gr/Cu.

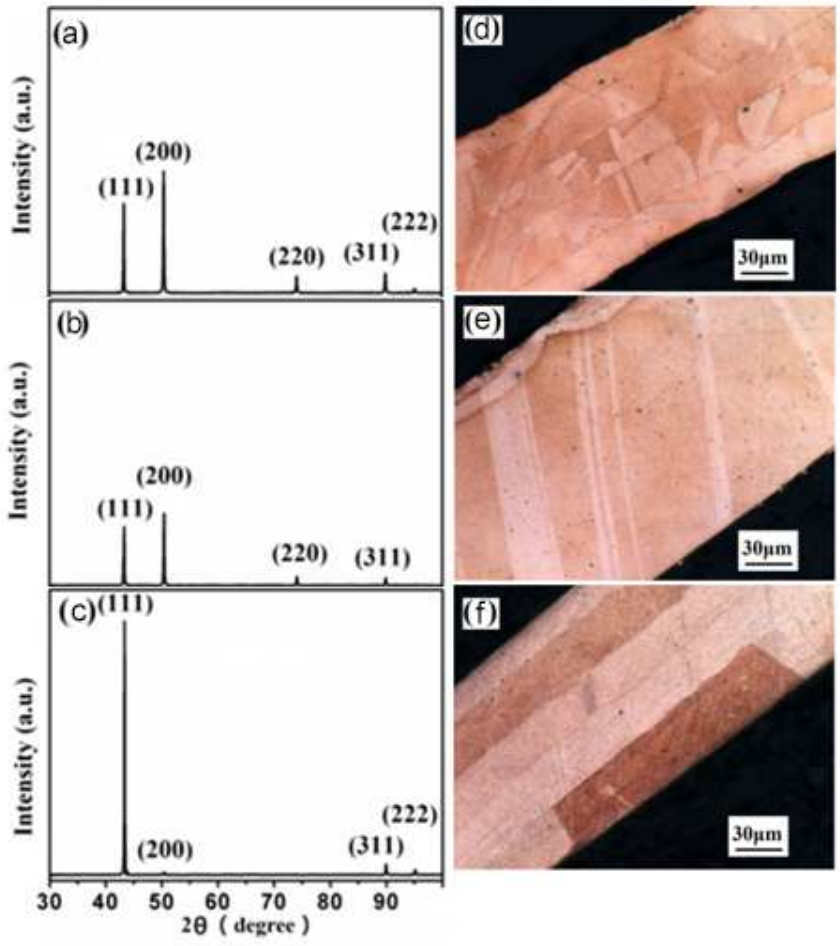

Figure S3

In-plane XRD patterns (left) and cross-section optical images (right) of hot-pressed multilayers of:
(a,d) pristine Cu,
(b,e) annealed Cu, and
(c,f) Gr/Cu.

Electrical Conductivity Measurement Details

The electrical conductivity measurement was carried out using a four-probe conductivity meter after the sample surfaces were carefully polished. The measuring principle diagram of the four-probe conductivity meter is shown in Figure S4.

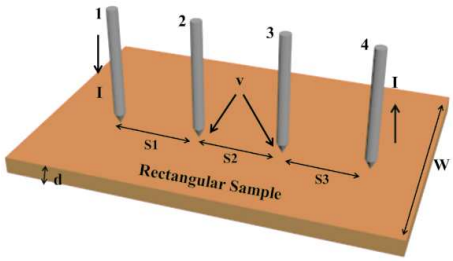

Figure S4. Schematic representation of the electrical conductivity measurement with the four-probe conductivity meter.

Before the actual measurement, the metal probes 1,2,3,4 were arranged in a straight line, and then pressed with a well-defined force onto the surface of the individual samples. When a current *I* appears between probe 1 and probe 4, a

corresponding potential difference V will be generated between probe 2 and probe 3. The material resistivity is then calculated according to the equation (1):

$$\rho = C\frac{V}{I} \qquad (1)$$

C is the probe correction factor for a sample with uniform resistivity and where the size of the sample satisfies the semi-infinite condition,

$$C = \frac{2\pi}{\frac{1}{S_1}+\frac{1}{S_2}-\frac{1}{S_1+S_2}-\frac{1}{S_2+S_3}} \qquad (2)$$

in which S1, S2, and S3 are the distances between probe 1-2, probe 2-3, and probe 3-4 respectively. Because the thickness of the thin sheet samples is close to the distance between the probes, (and thus does not conform to the semi-infinite boundary condition), a correction factor for the thickness, shape, and the probe position is required for the calculation.

The resistivity value can then be obtained by the following equation (3),

$$\rho = C\frac{V}{I} \cdot G\left(\frac{d}{s}\right) \cdot D\left(\frac{W}{s}\right) \qquad (3)$$

where $G\left(\frac{d}{s}\right)$ is the sample thickness correction function, and $D\left(\frac{W}{s}\right)$ is the sample shape and measuring position correction function. d is the thickness of the samples, W is the width of the rectangular sample, and S is the probe spacing ($\sim 1\text{mm}$).

Finally, the electrical conductivity can be calculated as 1/resistivity. In order to ensure the accuracy and reproducibility of the measurements, we used a precision wire-electrode cutting technique to cut the individual samples to exactly the same rectangular shape ($10 \times 5\text{mm}$) and thickness ($200\sim230\mu\text{m}$). The samples were polished with a 0.5 micron Al_2O_3 polishing powder in order to avoid any rough-surface-effects on the on conductivity measurement.

XPX and EDX Measurements

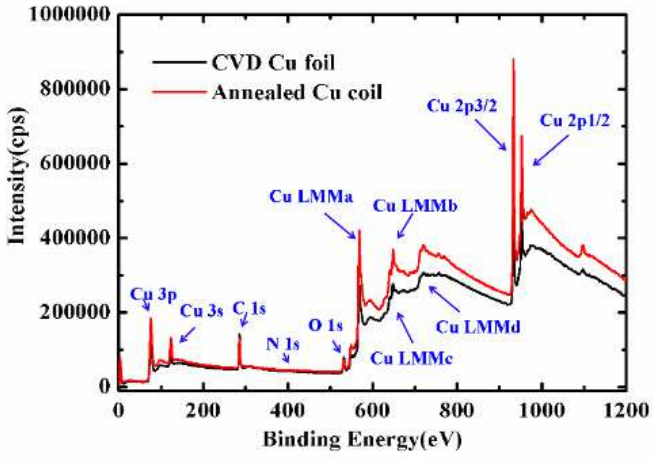

Figure S5 XPS data for the annealed Cu single foil (red), and Cu single layer foil with chemically deposited (CVD) graphene (black).

In order to verify the materials composition of the individual samples, we performed X-ray photoelectron spectroscopy (XPS) after CVD of graphene and after annealing of the reference samples. XPS is a surface-sensitive quantitative spectroscopic technique that measures the elemental composition. It was found that the

impurity content (i.e. surface contamination by mainly O, N) of the Cu samples with deposited graphene does not differ from the annealed Cu samples without graphene. It was also verified that the oxygen content had not changed after annealing or graphene deposition.

We have also performed energy-dispersive X-ray spectroscopy (EDX) for verifying the elemental composition of the samples. Similarly, the data did not indicate any change in the composition of the samples after CVD of graphene or after annealing. Therefore, we conclude that the observed change in the electrical conductivity was not caused by any surface contamination or change in material composition.

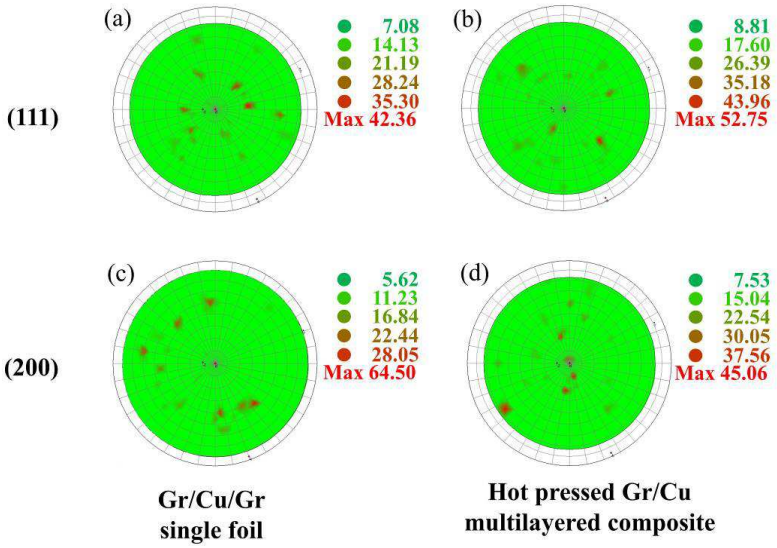

Figure S6. X-ray diffraction pole figures of (a) the (111) plane and (c) the (200) plane of the Gr/Cu/Gr single foil, and (b) the (111) plane and (d) the (200) plane Gr-Cu of the hot-pressed Gr/Cu multilayered composite. The intensities are color coded according to the tables on the right side of the individual pole figures with the respective maximum value shown in red.

Possible Graphene-Promoted Grain Re-orientation during the Hot-Pressing Process

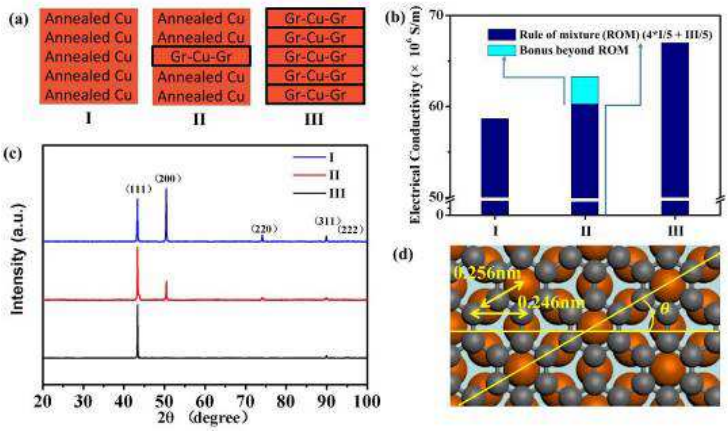

Figure S7
(a) Hot-pressed multilayered samples from (I) the annealed Cu foils, (II) one Gr-Cu-Gr foil sandwiched between several annealed Cu foils, and (III) the Gr-Cu-Gr foils. (b) Electrical conductivity values of the samples of I, II and III.

The sample II shows an electrical conductivity higher than that calculated from the rule of mixture based on the electrical conductivities of the samples I and III. (c) X-ray diffraction patterns indicate that sample II has a

transitional (intermediate) texture laying between that of sample I and II in terms of peak intensity ratio of $I_{(111)}/I_{(200)}$, suggesting a possible graphene-promoted grain re-orientation during the hot-pressing process because of the matching lattice constant (d) between graphene (2.46 Å) and Cu(111) (2.56 Å).

Customized Scanning Probe Device Integrated in SEM

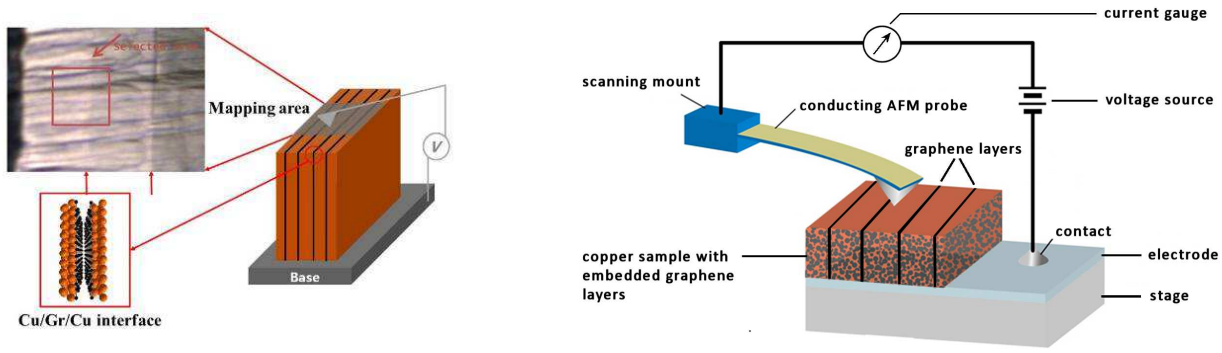

Figure S8
Schematic representation of the electrical properties measurement on the interface layers using the contact-current mode of a customized scanning probe microscope. A cantilever of an atomic force microscope is moved across the layered structure of the sample.

The scanning contact probe is built into the vacuum chamber of an SEM. A voltage is applied to the sample between the sample base and the cantilever probe. The probe is scanned across the "mapping area" to map the current flowing between probe and base. The sample is a multilayer 1cm x 1cm sandwich of Cu foils and interstitial graphene layers.

First-Principles Calculation Details

First-principles calculation was carried out using VASP code[1]. The Cu/Gr bilayer/Cu composite is modeled by an AB-stacked bilayer graphene which is sandwiched between fourteen Cu(111) layers as shown in Figure S10. The model system has a three-dimensional periodicity. The lattice constant of the Cu is 3.614 Å. The inter-layer distance of the AB-graphene is 3.430 Å, and the separation between the Cu and graphene is 2.210 Å, which is determined by minimization of the total energy. In calculations, the projector augmented-wave method[2] is used for the wave function expansion with an energy cutoff of 500 eV. The local density approximation is adopted for the electron exchange and correlation. The Brillouin zone is sampled with a 9 × 1 × 5 grid of the Monkhorst-Pack *k* points.[3] These calculation details were verified to provide accurate results.

Model System for the Cu/Gr Bilayer/Cu Composite

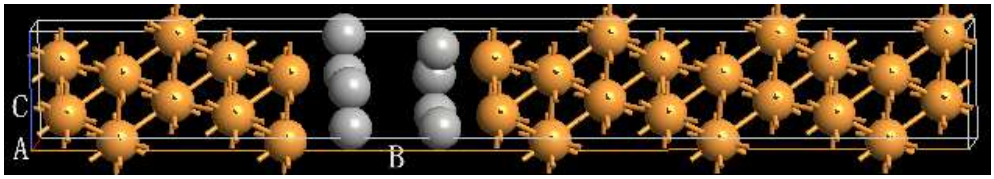

Figure S10
Model system for the Cu/Gr bilayer/Cu composite.

The yellow and grey spheres denote the Cu and C atoms, respectively. A, B and C denote the lattice parameters of this periodical model system, and they are arranged along the X, Y and Z axis, respectively.

We obtained the total charge of the Cu/Gr bilayer/Cu system and analyzed the Bader charge which is shown in Table S1. It shows that the graphene atoms have 32.480 valence electrons in total. The graphene obtained 0.480 electrons from the neighboring Cu atoms in total. It means that a primitive cell of the bilayer (containing four carbon atoms) is doped with 0.24 electrons. We also calculated the band structure and the density of states (see Figure 5 in the main text) of the AB-bilayer graphene using a primitive cell with 0.24 doping electrons by VASP. The lattice constant is 2.46 Å for the graphene. The Brillouin zone is sampled with a 21 × 21 × 1 grid of the Monkhorst-Pack *k* points.

Table S1 The valence charge of the AB-bilayer graphene sandwiched between the Cu(111) layers. X, Y and Z are the Cartesian coordinates of the graphene atoms. The graphene layers lie in the X-Z plane.

Atom type	No.	X	Y	Z	Charge
C	1	0.7988	11.6100	2.6749	4.1468
C	2	2.0769	11.6100	0.4612	4.1465
C	3	2.0769	11.6100	1.9370	3.9698
C	4	0.7988	11.6100	4.1507	3.9701
C	5	2.0769	14.9400	0.4612	3.9721
C	6	0.7988	14.9400	2.6749	3.9721
C	7	0.7988	14.9400	1.1991	4.1513
C	8	2.0769	14.9400	3.4128	4.1510

Theoretical Modelling Parameters

The first-principles calculation was carried out using VASP code.[30] The Cu/Gr bilayer/Cu interface was modeled by an AB-stacked graphene bilayer which was sandwiched between fourteen Cu(111) layers (see Figure S10 in the Supporting Information). The model system has a three-dimensional periodicity, and the lattice constant of the Cu(001) and graphene is 3.614 Å and 2.46 Å, respectively. The inter-layer distance of the AB-graphene is 3.430 Å, and

the separation between the Cu and graphene is 2.210 Å, which is determined by minimization of the total energy. In our calculations, the projector augmented-wave method[31] was used for the wave function expansion with an energy cutoff of 500 eV. The local density approximation was adopted for the electron exchange and correlation. The Brillouin zone was sampled in the *k* space with the Monkhorst-Pack scheme.[32]

References of the Supporting Information

[1]. G. Kresse, J. Furthmüller, *Phys. Rev. B*, **1996,** *54*, 11169.
[2]. P.E. Blöchl, *Phys. Rev. B*, **1994,** *50*, 17953.
[3]. H.J. Monkhorst, J. D. Pack, *Phys. Rev. B,* **1976***, 13,* 5188.

Amendment 1

A Possible Route for Mass-Production of Graphene-Cu Composites

Commercial copper powder (a) was converted to copper flake powder (b) by a ball-milling process. The thickness of the copper flakes could be controlled in the range of several hundred nanometers to tens of micrometers by adjusting the ball-milling time (for example 1, 3 and 7 hours as shown in (b)). Then graphene (Gr) was deposited on the surface of the copper flakes by chemical vapor deposition (c). The graphene (Gr) was homogenously deposited on the surfaces of the flakes. The number of layers of the deposited graphene could be controlled by adjusting the carbon source concentration. Bulk composite samples were made by self-assembling and solidifying the graphene-coated copper flakes. TEM analyses reveal that a uniform nanolayered structure was obtained (d). The insert SEM image in (c) is the fractured surface morphology of the Gr-Cu composite clearly showing a nanolayered structure.

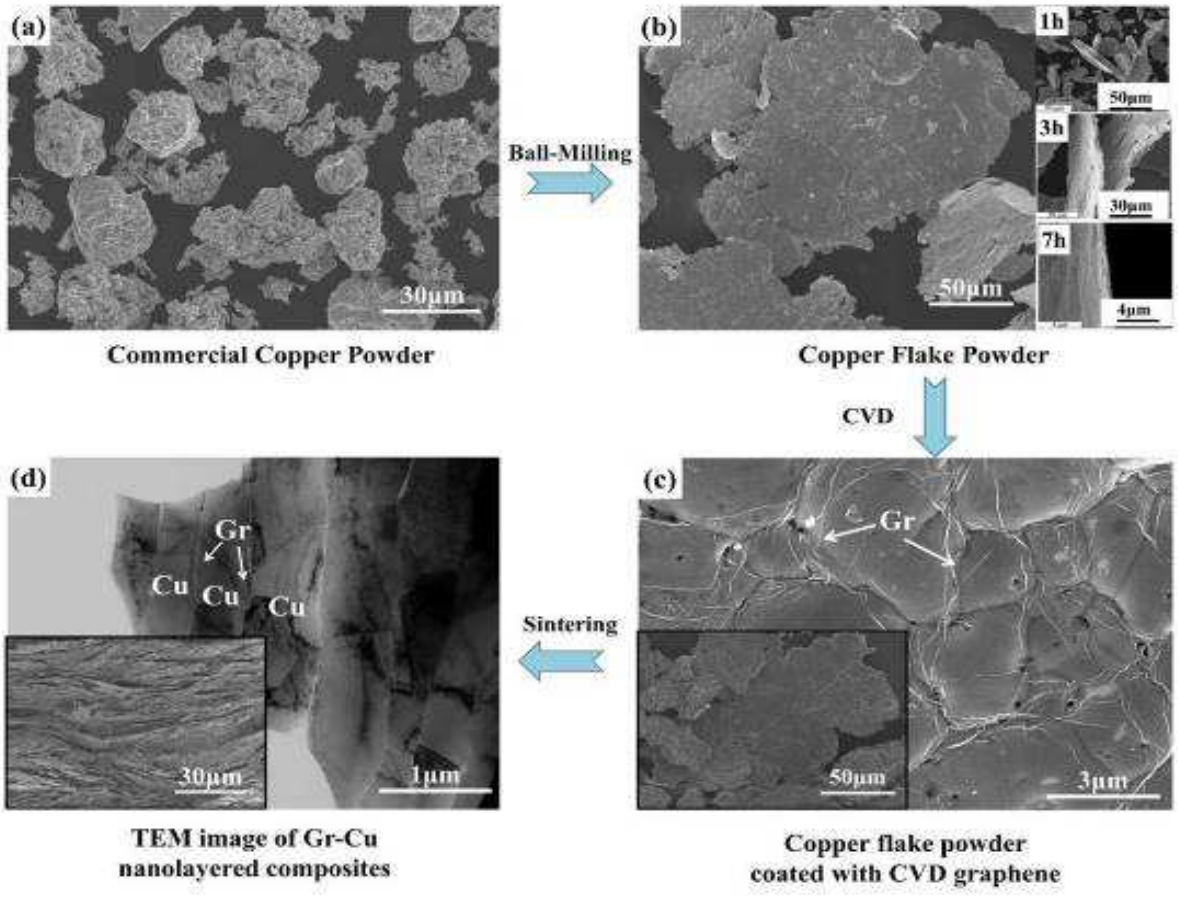

Figure A1.1 Fabrication route for graphene-Cu matrix composites with a bioinspired nano-layered structure